

流化床床料与燃煤颗粒的形貌分析

刘柏谦, 苏伟强, 洪 慧, 王立刚

(北京科技大学机械工程学院, 北京 100083)

摘 要: 测量了一台循环流化床锅炉宽筛分原煤和冷渣的颗粒形貌, 研究了球形度、Zingg 指数、分形分数的变化, 关联了 Wadell 球形度和 Krumbein 球形度之间的换算关系。研究表明, 宽筛分煤燃烧后的冷渣比原煤具有更强烈的非线性特征。采用当量体积直径与 Wadell 球形度和 Krumbein 球形度的关联都是集中到某一个区域范围的散点图; 采用扁平度、伸长度和 Zingg 指数为指标的颗粒形貌分布显示多数颗粒形貌以片状颗粒为主; 采用分形维数进行的颗粒描述显示, 大颗粒和小颗粒的分形维数不同, 大小颗粒的分界点对原煤约为 3.17 mm, 冷渣约为 3.06 mm。

关 键 词: 流化床; 床料; 煤颗粒; 颗粒形貌; 片状

中图分类号: TK224.1 文献标识码: A

引 言

流化床燃烧技术已经有半个多世纪的发展历史, 半个多世纪的发展过程中, 已经形成比较完整的设计方法和研究手段。不论从燃烧学还是流态化理论, 描述流化床操作过程的物理描述和数学描述都比较完善。燃烧过程的描述(如挥发分析出时间、单颗粒燃烧时间)和流态化过程描述(床层压降、临界流化速度、颗粒运动特征)广泛使用颗粒度的概念。而实际工程中, 流化床燃烧都是采用宽筛分床料和燃料, 颗粒度的测量是采用筛分方法, 即用连续或不连续的多个筛子对颗粒群进行筛分, 然后称量每个筛子上的残留重量作为权重, 乘积求和就可以获得颗粒度数值。有些国家如中国, 还要求将结果乘以颗粒球形度。这样得到的颗粒度与计算公式中的颗粒度在物理意义上可能存在一定的差异, 几乎所有的计算公式中都将研究对象看作是球形颗粒, 如果认为是非球形颗粒, 则引进球形度因子进行修正。为了描述颗粒形貌的影响, 已经建立了许多指标, 如形状指数、形状因子, 每个指标有包含若干个具体定义。

为了研究非球形颗粒在气固体系中的行为, 进而定量描述气固体系的宏观特征, 已经大量研究了各种各样的气固颗粒体系。Brown 得到了颗粒填充空隙率与球形度的关系图^[1]。R. P. Zou & A. B. Yu 在更宽的范围得到了颗粒的填充空隙率与球形度的关系^[2], 并提出了拟合方程, 所得结果已包含了 Brown 的数据范围。Heiss & Coull 得出了圆柱形颗粒蠕流状态下动力形状因子与球形度的关系式^[3](参见文献[4])。Dolejs & Machac 提出了非球形颗粒的固定床压降方程^[4]。Yoshiyaki Endo 等人提出了层流区多分散系非球形颗粒固定床压降方程^[5]。Fridrun 评价了描述颗粒粗糙度和球形度的三维形状因子^[6]。Chhabra 及其合作者连续评价了非球形颗粒在各种系统中的流动阻力^[7~12]。M. Eriksson 评价了伸长度、Heywood 形状系数和长宽比^[13]。Anneke M. B. 研究了长宽比、圆形度、投影形状因子、形状因子、平面临界稳定性、径向形状因子、斯托克斯形状因子、质量形状因子和粗糙度因子等 9 种颗粒形貌定义并进行了评价^[14]。

很多流化床都燃用宽筛分燃料, 这些大小不同的颗粒不仅在流化床中有不同的燃烧效果, 在流化床中的运动状态也大相径庭。流化床燃烧的床料中主要是较大颗粒的灰渣。按照燃烧的煤质和筛分特性, 燃煤占流化床床料的质量介于 2%~5% 之间。虽然燃煤的数量不多, 但由于流化床锅炉要求连续运行, 燃烧之后的灰渣在流化床中停留时间较长, 而床料是连续地排出流化床, 这样, 所有大于某一尺寸的颗粒都可以在较长的时间内以灰渣的身份在流化床内停留。因此, 煤颗粒和灰渣颗粒的形貌演化对流化床燃烧和流态化有着重要的影响。为了研究这种影响, 以一台 50 MW 循环流化床锅炉及其燃用得片状特征明显的京西无烟煤为研究对象, 分别选取一定量的煤颗粒和冷渣颗粒, 研究流化床燃烧过程

收稿日期: 2006-06-01; 修订日期: 2006-09-01

基金项目: 国家自然科学基金资助项目(50476082)

作者简介: 刘柏谦(1958-), 男, 吉林人, 北京科技大学教授。

造成的颗粒形貌变化。锅炉的基本情况见文献[15~16]。

1 颗粒形状与球形度、Zingg 指数

1.1 颗粒形状和球形度

颗粒的几何性质包括大小、形状、表面结构和孔结构等。几何性质对颗粒群的许多性质都有影响, 例如: 比表面积、流动性、填充性、化学活性等。颗粒形状是指一个颗粒的轮廓或表面上各点所构成的图像。由于颗粒形状千差万别, 描述颗粒形状的方法可分为两类: 语言术语和数学术语。尽管某些术语并不能精确描述颗粒形状, 但它们大致反映了颗粒形状的某些特征。为了描述颗粒的形状, 需要采用一些具体指标, 习惯上将颗粒大小的无因次组合称为形状指数(shape index), 立体几何各变量的关系则定义为形状系数(shape factor), 统称为形状因子。

形状指数中, 球形度是一个使用广泛的参数, 它描述了非球形颗粒与球形颗粒之间的形状差异。球形度有多种定义, Wadell 球形度作为基本定义, 虽然使用不方便, 但由于物理意义明确、定义简单, 还是得到广泛应用。另一种球形度, Krumbein 球形度由于可以经过简单测量就可以计算出数值, 使用起来比较方便。

Wadell 球形度的定义为:

$$\varphi_w = \frac{\text{与颗粒体积相等的球体表面积}}{\text{颗粒表面积}} = \frac{\pi d_V^2}{S} \quad (1)$$

Krumbein 球形度为:

$$\varphi_K = 3 \sqrt[3]{\left(\frac{h}{b}\right) \left(\frac{h}{l}\right)^2} \quad (2)$$

1.2 Wadell 球形度与 Krumbein 球形度之间的关系

为了研究两种球形度之间的关系, 首先选择规则形状颗粒进行研究, 这样就避开了测量非球形颗粒表面积和体积的复杂过程, 研究结果可作为非球形颗粒的参照物。以圆柱形颗粒为例, 设圆柱直径为 1, 颗粒的高度由 0.01~10 变化, 按照颗粒 Wadell 球形度和 Krumbein 球形度的定义可以得出两种球形度随圆柱和方柱体高度的变化, 如图 1 和图 2 所示。

当圆柱的高度为 1 时(颗粒高度等于圆柱直径), Wadell 球形度取得最大值(小于 0.873 5); 大于 1 时, Wadell 球形度逐渐减小, 但减小趋势较缓慢。Krumbein 球形度在颗粒高度 0.55 取得最大值(~0.9); 小于 0.55 几乎为线性增加, 在大于 0.6 以后

急剧减小。从直觉上, 当颗粒的高度小于圆柱的直

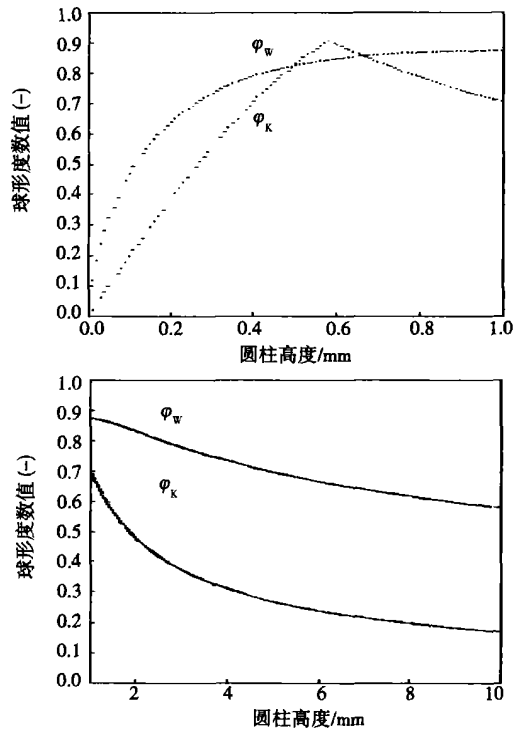


图 1 圆柱形颗粒 Wadell 球形度和 Krumbein 球形度的比较

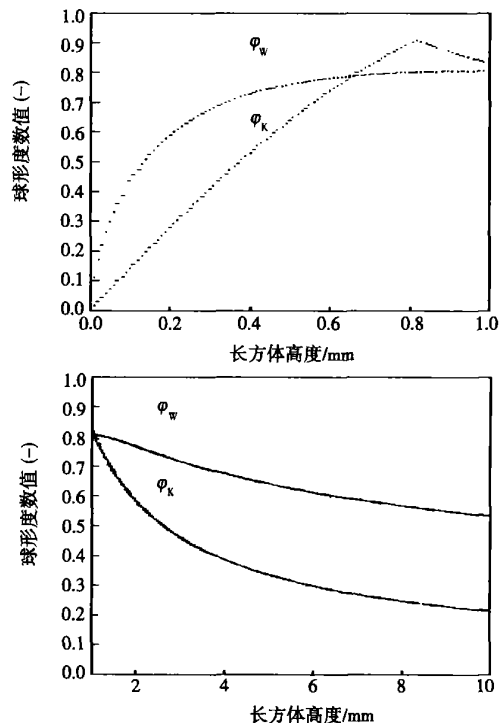


图 2 长方体颗粒 Wadell 球形度和 Krumbein 球形度的比较

径(为1)时,可视为片状,而厚度大于直径时,可视为呈棒状。从两种球形度随颗粒高度的变化趋势上看,两着都有极值,但极值点不同,出现的颗粒高度不同。

还有一个重要的现象,两个颗粒的形状不同却可以有相同的球形度。如当颗粒呈片状时球形度0.75对应着3个球形度。只有在Wadell球形度小于0.55或Krumbein球形度小于0.8时球形度和颗粒形状才会一一对应。这意味着不能单纯用球形度来判断颗粒的形貌。此外,图中可还可以看到片状颗粒球形度随颗粒厚度变化较快,而棒状颗粒的球形度随颗粒长度变化较缓。

图2是两种球形度随正方形截面颗粒高度增减的变化曲线。正方形截面颗粒与圆形截面颗粒两种球形度的变化趋势完全相同,但球形度极值和极值发生点不同。Wadell球形度也是在颗粒高度与正方形底边边长相等时,取得最大值(0.8)。Krumbein球形度在颗粒高度小于0.8附近,取得最大值(大于0.9),图3给出了两种球形度之间的关系。

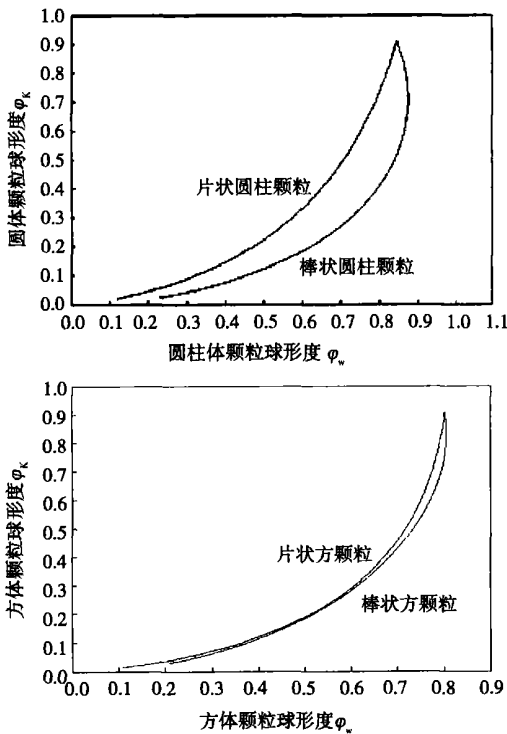


图3 圆柱和方体颗粒两种球形度的相互关系

由于Krumbein球形度只需测量颗粒的3个外形尺寸,就可以简单地换算出Wadell球形度。

圆柱片状:

$$\varphi_w = 1.33\varphi_k^3 - 2.81\varphi_k^2 + 2.28\varphi_k + 0.11 \quad (3)$$

圆柱棒状:

$$\varphi_w = 3.88\varphi_k^3 - 6.42\varphi_k^2 + 3.55\varphi_k + 0.16 \quad (4)$$

长方片状:

$$\varphi_w = 1.65\varphi_k^3 - 3.39\varphi_k^2 + 2.47\varphi_k + 0.13 \quad (5)$$

长方棒状: $\varphi_w = 2.65\varphi_k^3 - 4.52\varphi_k^2 + 2.76\varphi_k + 0.14 \quad (6)$

1.3 Zingg 指数

Zingg 指数是一种定义简单的颗粒形貌描述指标,其定义为颗粒长宽度和扁平度之比,即:

$$F_z = N / M = LT / B^2 \quad (7)$$

式中: N —长宽度, $N = \text{长径} / \text{短径} = L / B$; M —扁平度; $M = \text{短径} / \text{高度} = B / T$; L, B, T —按Heywood规定测量的颗粒长宽高。

由定义可知,可以综合考虑颗粒的球形度与Zingg指数,来判断颗粒的形状。 $F_z > 1$ 时,颗粒应属于棒状, F_z 越大,颗粒越细长,球形度越小; $F_z < 1$ 时,颗粒应该属于片状, F_z 越小,颗粒的片状化越严重,球形度也越小。

2 流化床燃烧颗粒的分维数

煤是流化床燃烧的主要燃料,冷渣是流化床燃烧后排出的产物,它们都是形态不规则的固体颗粒。燃煤和冷渣的颗粒形貌对流化床锅炉的流化、燃烧、传热都有着重要的影响,本研究从流化床锅炉采样获得了原煤与燃烧后冷渣样品,通过实验测量和计算获得了颗粒的粒度数据,用常规的形状因子法分析了颗粒形貌的变化,并用非线性数学的分维方法分析了煤及冷渣颗粒的粒度分维变化。

2.1 颗粒形貌的形状因子分析

从循环流化床锅炉燃料和冷渣取颗粒样品,通过四分法取样筛分后各取333颗颗粒,颗粒选取以满足手工测量外形尺寸为标准。为使Wadell球形度和Krumbein球形度的比较有统一标准,采用体积等效半径作为两种球形度比较的媒介。

图4是煤颗粒和冷渣颗粒两种球形度随等效半径变化的散点图。可以看出,两种球形度分布随等效半径无明显规律,但是燃烧前后,颗粒的球形度发生了变化。煤粒的Wadell平均球形度0.76,冷渣的Wadell平均球形度0.71;煤粒的Krumbein平均球形度0.2,冷渣的Krumbein平均球形度0.1。所以说:煤粒燃烧成为冷渣颗粒后,球形度有所降低,即增加了片状化倾向。此外,从数值上,Wadell球形度大于Krumbein球形度,这与前面我们研究圆柱片状颗粒的两种球形度差别的结果是一致的。由于Wadell

球形度是通过颗粒的三维尺寸等效成长方体计算得出, 相当于增加了颗粒的面积和体积, 严格意义上,

Wadell 球形度的数值是不准确的。表 1 是煤颗粒和冷渣颗粒球形度与等效半径的统计平均值。

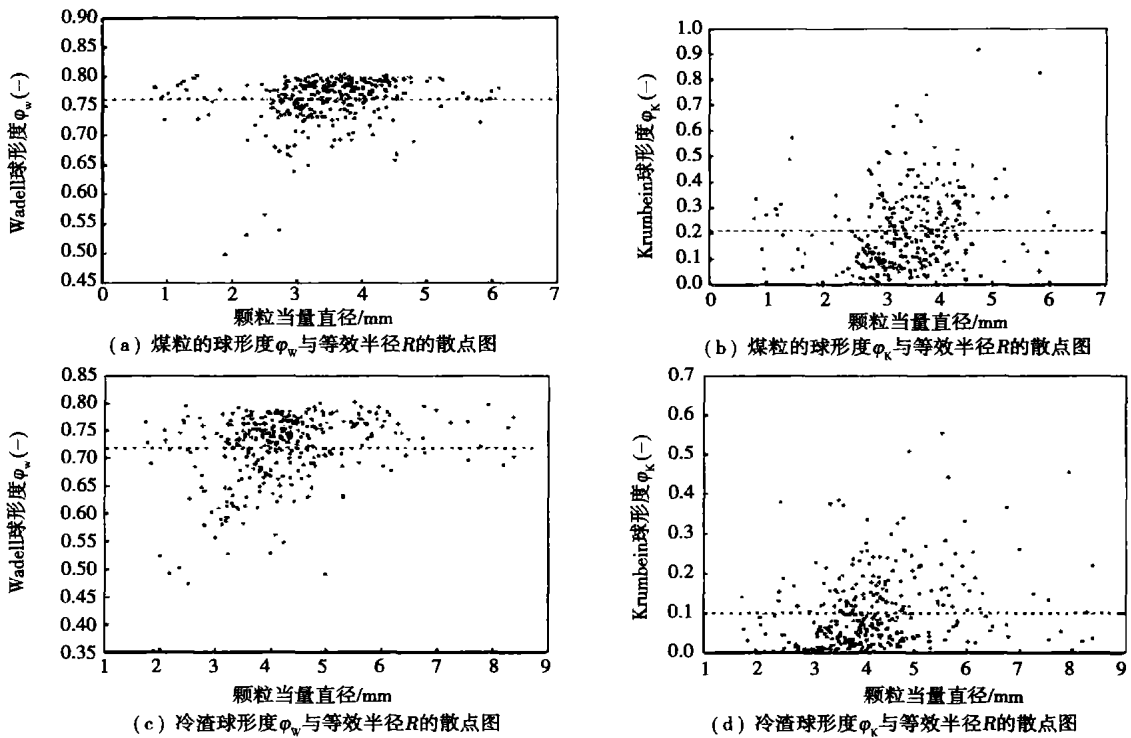


图 4 颗粒球形度与当量直径的测量值

利用前面对圆柱片状和长方片状的研究关系式从测得的 Krumbein 球形度转换成 Wadell 球形度, 其数值也列于表 1 中, 可以看出, 转换后颗粒的 Wadell 明显小于普通煤粉的球形度的数值 (0.6 ~ 0.62)。

表 1 煤和冷渣颗粒的平均球形度和平均等效半径

	$\bar{\varphi}_k$	$\bar{\varphi}_w$	长方片状 $\bar{\varphi}_w$	圆柱片状 $\bar{\varphi}_w$	R
煤粒	0.209 776	0.761 442	0.514	0.477	3.457
冷渣颗粒	0.100 17	0.718 246	0.345	0.312	4.145

将燃煤颗粒按长短度和扁平度分类来查看颗粒的形态, 如图 5 所示。可以看出燃煤颗粒以等维体和碟状颗粒占大多数, 板状和棒状颗粒较少。如果按照 Zingg 指数分成片状和棒状, 则片状颗粒约占一半的份额, 说明这种燃煤有较大的片状化趋势。

2.2 颗粒粒度分布的分维分析

分维分析是研究在各种尺度下不规则、不光滑物体的一种有效手段。采用盒维数法研究上述两组颗粒的粒度分维。盒维数定义为:

$$N(r) = G^{-D} \tag{8}$$

将上式两边取对数, 则有:

$$\lg N = m - D \lg r \tag{9}$$

在 $\lg N - \lg r$ 的双对数图上, 斜率的绝对值即为粒度分维值。特征尺寸 r 采用颗粒的等效半径 R , 对煤及冷渣颗粒的数目—等效半径关系统计见表 2, 相应的曲线见图 6。从图中可以看出, 煤粒及冷渣颗粒的粒度分维的关系图并非为一条直线, 而是两条分段直线, 煤粒在等效半径 $R = 3.17 \text{ mm}$ ($\lg R = 0.501$) 处, 冷渣在等效半径 $R = 3.06 \text{ mm}$ ($\lg R = 0.485$) 处存在折弯点, 在小尺度时, 分维值较小; 在

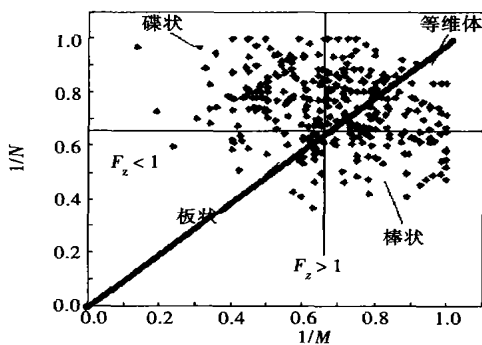


图 5 燃煤颗粒形态分布

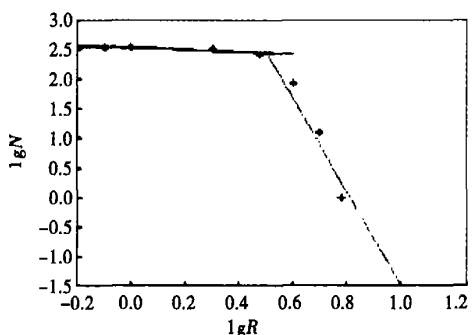
大尺度时,分维值较大(见表 3)。

表 2 颗粒一半径分布统计

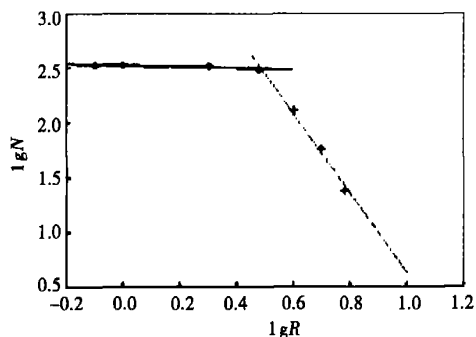
数目 <i>N</i>	半 径 <i>R</i>						
	> 0.8 mm	> 1 mm	> 2 mm	> 3 mm	> 4 mm	> 5 mm	> 6 mm
煤粒	333	329	316	253	81	12	1
煤灰	333	333	328	303	180	58	24

表 3 不同尺度下的煤和冷渣颗粒的粒度分维

	D_1	D_2
煤颗粒	0.182 82 ($R < 3.17$ mm)	7.821 3 ($R > 3.17$ mm)
冷渣颗粒	0.063 5 ($R < 3.06$ mm)	3.612 9 ($R > 3.06$ mm)



(a) 煤颗粒的粒度分维



(b) 冷渣颗粒的粒度分维

图 6 颗粒分形维数的测量值

李霜研究了煤粉锅炉粉煤灰的粒度分维, 它的结果得到了单一的分维值^[17]。谢和平介绍了 Cohen & Knight 测量土样本的表面分维时, 一种土样本被分成两组, 一组为精细粒子, 一组为粗糙粒子, 分别得到了两个分维值^[18]。G. W. Stachowiak 研究磨损颗粒的形状分维时, 在不同尺度下, 也存在两个分维值, 称小尺度下的分维为 textual fractals dimension, 而称大尺度下的分维为 structural fractals dimension^[19]。因此, 对于颗粒的分维研究, 小尺度与大尺度存在着

不同的分维特征, 无论是粒度分维、形状分维、还是表面积分维都存在这种现象。本研究的流化床颗粒粒度比土壤和粉煤灰大一个数量级, 筛分范围比较宽, 粒度特征在小尺度范围和大尺度范围呈现不同的分维特征。同时也显示出, 虽然按照经典指标的测定结果显得比较分散, 但采用简单的分维处理后, 颗粒之间非线性特征就比较清晰地显示出来了。

由表 3 的粒度分维值可看出: 无论在小尺度, 还是在大尺度下, 冷渣的分维值要小于煤的分维值。虽然郁可、G. W. Stachowiak 和薛祥立等人都认为煤粉粒度分维数是衡量煤粉颗粒细度与均匀性的重要指标^[20~21], 分维数愈大, 煤粉颗粒愈细愈均匀, 煤粉颗粒分布愈集中, 但宽筛分的流化床燃烧与煤粉表现出了不同的分形特征, 而且原煤的分形与冷渣的分形也有数值上的差别。

3 结 论

宽筛分燃煤流化床床料主要由灰渣组成, 占床料质量份额 95% 以上的惰性床料对流化床流体动力特性有着重要影响, 而这些数量庞大的床料是由占床料总量 2% ~ 5% 原煤经过燃烧演化而成。因此, 原煤颗粒的形貌特征决定了床料的颗粒特征。

对宽筛分京西无烟煤及其循环流化床冷渣进行的形貌研究显示, 采用当量体积直径与 Wadell 球形度和 Krumbein 球形度的关联都是集中到某一个区域范围的散点图; 采用扁平度、伸长度和 Zingg 指数为指标的颗粒形貌分布, 显示多数颗粒形貌一片状颗粒为主; 采用分形维数进行的颗粒描述显示, 大颗粒和小颗粒的分形维数不同, 原煤的分形维数大于冷渣的分形维数。大小颗粒的分界点对原煤约为 3.17 mm, 冷渣约为 3.06 mm。这些形貌描述, 对进一步研究流化床燃烧过程和流体动力行为由一定的参考价值。

参考文献:

- [1] BROWN G G. Unit Operations[M]. New York: Wiley, 1950.
- [2] ZOU R P, YU A B. Evaluation of the characteristics of mono-sized non-spherical particles[J]. Power Technology, 1996, 88: 71-79.
- [3] HEISS J F, COULL J. The effect of orientation and shape on the settling of non-isometric particles in a viscous medium[J]. Chem Eng Prog, 1952, 48(3): 33-140.
- [4] DOLEJE V, MACHAC I. Pressure drop during the flow of newtonian fluid through a fixed bed of particles[J]. Chemical Engineering and Processing, 1995 34: 1-8
- [5] YOSHIYUKI ENDO, CHEN DA REN, DAVID Y H PUI. Theoretical

- consideration of permeation resistance of fluid through a particle packed layer[J]. *Power Technology*, 2002, 124: 119—126.
- [6] FRIDRUN PODCZECK, NEWTON M J. The evaluation of a three-dimensional shape factor for the quantitative assessment of the sphericity and surface roughness of pellets[J]. *Int J of Pharmaceutics*, 1995, 124: 253—259.
- [7] MADHAV VENU G, CHHABRA P R. Drag on non-spherical particle in viscous fluids[J]. *Int J Miner Process*, 1995, 43: 15—29.
- [8] FERREIRA J M, CHHABRA R P. Accelerating motion of a vertically falling sphere in incompressible newtonian media: an analytical solution [J]. *Powder Technology*, 1998, 97: 6—15.
- [9] RAJITHA P, CHHABRA P R, SABILI N E, et al. Drag on non-spherical particles in power law non-newtonian media[J]. *Int J Miner Process*, 2006, 78: 110—121.
- [10] CHHABRA R P, KIRTI RAMI, UHLHERR P H T. Drag on cylinders in shear thinning viscoelastic liquids[J]. *Chemical Engineering Science*, 2001, 56: 2221—2227.
- [11] CHHABRA R P, AGARWAL L, SINHA N K. Drag on non-spherical particles: an evaluation of available methods[J]. *Powder Technology*, 1999, 101: 288—295.
- [12] NITIN S, CHHABRA R P. Non-isothermal flow of a power fluid past a rectangular obstacle in channel: drag and heat transfer[J]. *Int J of Engineering Science*, 2005, 43: 707—720.
- [13] ERIKSSON M, ALDERBORN G, NYSTROM C, et al. Comparison between and evaluation of some methods for the assessment of the sphericity of pellets[J]. *Int J of Pharmaceutics*, 1997, 148: 149—154.
- [14] ANNEKE M BOUWMAN, JAAP C BOSMA, PIETER VONK, et al. Which shape factor best describe granules[J]. *Powder Technology*, 2004, 146: 66—72.
- [15] 刘柏谦. 片状化石燃料的循环流化床燃烧[J]. *北京科技大学学报*, 2005(2): 159—163.
- [16] 刘柏谦. 片状化石燃料的循环流化床燃烧[J]. *北京科技大学学报*, 2005(4): 418—422.
- [17] 李 霜, 李焕英, 李启令. 粉煤灰颗粒群几何特征的图象分析研究[J]. *建筑材料学报*, 2001(3): 49—54.
- [18] 谢和平. 分形—岩石力学导论[M]. 北京: 科学出版社, 1996.
- [19] STACHOWIAK G W. Numerical characterization of wear particles morphology and angularity of particles and surfaces[J]. *Tribology International*, 1998, 31: 139—157.
- [20] 郁 可. 粉体粒度分布的分形研究[J]. *材料研究学报*, 1995(6): 39—43.
- [21] 薛祥立. 粒度分布函数的分形表示[J]. *青岛建筑工程学院学报*, 1997(4): 24—29.

(辉 编辑)

新 产 品

用于 20 ~ 40 MW 燃气轮机的新行星齿轮箱

据《Gas Turbine World》2006 年 7 ~ 8 月号报道, 拉脱维亚市政供热公司为城市生产 48 MW 电力和 50 MW 分区供热。用于整套承包的供货范围包括 1 台 32.1 MW Rolls-Royce RB211—6761 干式低排放燃气轮机和 1 台 16 MW 汽轮机, 被结合进一个单升箱装体。

项目工程师说, 能够把燃气轮机和汽轮机组结合进一个单升箱装体是由于行星齿轮箱重量和尺寸的减少。Allen Gears 公司的大功率行星齿轮减速箱把燃气轮机额定输出转速 4 800 r/min 减少到用于 50 Hz 电力生产的 1 500 r/min。

该行星齿轮减速箱重约 5 t, 而与之对应的传统的平行轴减速齿轮箱的重量却超过 7 t。齿轮箱横截面积是相应的平行轴装置的一半。

Allen 把它的行星齿轮同轴装置组装为一种标准的底座安装设计; 并针对空间受限的应用, 组装为发电机安装的设计。这种方案具有竞争的优势, 因为平行轴齿轮箱只能用作偏置的底座安装设计。

对于近海的工程项目, 空间和重量始终是很受重视的, 减少的尺寸和重量使行星齿轮箱具有明显的优势。

底座安装的优点包括易于拆卸以便进行检查和改变齿轮传动比、更加简化的接口、无障碍地接近涡轮机和发电机。

发电机安装的优点包括减少齿轮箱—涡轮机任何潜在的不对中问题, 并便于对整套涡轮机—发电机组件的验收试验。

此外, 发电机安装的设计排除了对于大型高扭矩的齿式和挠性联轴器的需要。

发电机安装也提供了共用公用的发电机—齿轮箱润滑油系统选择的余地。

(吉桂明 供稿)

基于支持向量机的锅炉过热系统建模研究 = **A Study of the Modeling of a Boiler Superheating System Based on a Supportive Vector Machine** [刊, 汉] / LIU Sheng, LI Yan-yan (College of Automation under the Harbin Engineering University, Harbin, China, Post Code: 150001) // Journal of Engineering for Thermal Energy & Power. — 2007, 22(1). — 38 ~ 41

Due to such features as a strong non-linearity and time-variation etc. specific to a boiler superheating system, it is very difficult to establish a mathematical model for the latter by using a conventional method. Hence, the authors have proposed a method for modeling a boiler superheating system based on a supportive vector machine and process mechanism. By making use of the relevant training data produced by a mechanism model, one can use the proposed method to train a network of the supportive vector machine, enabling the network to very well approximate to the non-linear model of the superheating system and in the meantime to utilize irrelevant data samples to verify its generalized performance. It can be seen from the simulation results that the network of the supportive vector machine will converge after 3.18 seconds when it has been optimized by using an inner point method. The maximal error of the learning process will not exceed 0.035 °C. Consequently, the method can be used to effectively build a model for a system with a high simulation accuracy and is suited for modeling not only a superheating system but a whole boiler system. **Key words:** boiler, superheating system, supportive vector machine, mechanism model

基于数据融合的燃料量软测量及煤质发热量在线校正 = **Soft Measurement of Fuel Quantity Based on Data Fusion and On-line Calibration of Coal Heat Values** [刊, 汉] / ZHAO Zheng, LIU Ji-zhen, TIAN Liang (Education Ministry Key Laboratory on Power Plant Equipment Condition Monitoring and Control, North China University of Electric Power, Baoding, China, Post Code: 071003) // Journal of Engineering for Thermal Energy & Power. — 2007, 22(1). — 42 ~ 45, 60

To guarantee the accuracy and reliability of fuel quantity measurement, a method for soft measurement of fuel quantity is presented based on data fusion. A model for the soft measurement of fuel quantity has been established mainly through an analysis of the measured values relating to fuel quantity and a statistical analysis of on-site operation data. The data from several sensors were processed by using the data fusion technique, effectively enhancing the accuracy of the data from the soft measurement. The model for soft measurement of fuel quantity established through a simulation verification can reflect comparatively well the change in actual fuel quantity, improving the safety and reliability of the whole system. Meanwhile, taking into consideration the status quo of time-related variation of coal quality and through a statistical analysis of the elements and industrial analytic results of 56 kinds of coal, one can find out the relation between the low heat value and theoretical air quantity as well as the relation between the water and ash content in coals on an as received basis on the one hand and the fuel low heat value on the other. Two methods for an on-line calibration of fuel low heat values are thereby presented. With the change in the low heat value representing a change in coal quality, the coal-air ratio can be optimized, thus providing an on-line basis of coal quality changes for performance calculations and combustion optimization. **Key words:** soft measurement, data fusion, fuel quantity, low heat value

流化床床料与燃煤颗粒的形貌分析 = **Morphological Analysis of Fluidized Bed Materials and Raw Coal Particles** [刊, 汉] / LIU Bai-qian, SU Wei-qiang, HONG Hui, et al (College of Mechanical Engineering under the Beijing University of Science and Technology, Beijing, China, Post Code: 100083) // Journal of Engineering for Thermal Energy & Power. — 2007, 22(1). — 46 ~ 51

The morphology of raw coal and cold cinder particles sifted through a wide-mesh screen from a circulating fluidized bed boiler has been measured along with a study of the change in sphericity, Zingg exponent and fractal fraction. Correlated was the conversion relation between Wadell and Krumbein sphericity. The study shows that the cold cinder produced by the combustion of coal sifted through a wide-mesh screen has non-linear characteristics stronger than those of raw coal. If an equivalent volumetric diameter is employed, its correlation with Wadell and Krumbein sphericity has all been concentrated to a scattering point chart in a certain zone range. Morphological particle distribution in case of using flatness elongation and Zingg exponent to serve as indexes will exhibit a morphological appearance of a great majority of particles, in

which flaky particles predominate. The description of particles by using fractal dimensions will show different fractal dimensions for large particles and small ones. The boundary dividing point of big and small particles is about 3.17 mm for raw coal and about 3.06 mm for cold cinder. **Key words:** fluidized bed, bed materials, coal particle, particle morphological appearance, flaky shape

循环流化床锅炉飞灰残碳的生成及其处理 = **Formation of Fly-ash Carbon Residue in a Circulating Fluidized Bed Boiler and Its Disposal** [刊, 汉] / LI Shao-hua, WANG Qi-min, XIAO Xian-bin, et al (Thermal Energy Department, Tsinghua University, Beijing, China, Post Code: 100084) // Journal of Engineering for Thermal Energy & Power. — 2007, 22(1). — 52 ~ 56

Circulating fluidized bed combustion techniques have been widely used in China due to its numerous merits. However, a universal problem in operation is that the carbon content of fly-ash is much higher than generally expected. The major factors influencing the carbon content of fly ash are: coal index, coal structure and coke reaction activity, feed-coal particle diameter and structure of the circulating fluidized bed as well as other operational parameters etc. At present, the methods for reducing fly-ash carbon content mainly include: fly ash recirculation, secondary air strength enhancement and pressure-drop adjustment for a circulating fluidized bed etc. The experiments performed by the authors indicate that under the condition of a low air speed, the carbon residue in fly ash can be fully burnt up. In addition, high voltage electrostatic separation and fly-ash water activated agglomeration can also provide a new approach for utilizing carbon residue in fly ash. **Key words:** circulating fluidized bed boiler, carbon content of fly ash, low speed circulating fluidized bed, electrostatic separation, fly-ash water activated agglomeration

撞击气化火焰边缘的分形特性 = **Fractal Characteristics of an Impinging Gasification-flame Edge** [刊, 汉] / LIANG Qin-feng, NIU Miao-ren, YU Guang-suo, et al (Clean Coal Technology Research Institute under the East China University of Science and Technology, Shanghai, China, Post Code: 200237) // Journal of Engineering for Thermal Energy & Power. — 2007, 22(1). — 57 ~ 60

A gasification furnace is a key equipment item in an IGCC (integrated gasification combined cycle) power generation system. During tests, the authors have by using a flame camera system taken the pictures of impinging gasification-flames in a multi-nozzle and opposed gasification furnace. The fractal dimension of the impinging gasification-flame edge was calculated by using a pixel-covering method, providing an effective method for judging the combustion condition of the impinging gasification-flame. The test results show that the curves of the above-mentioned flame edge assume fractal characteristics. The fractal dimensions of the flame edge curve will gradually decrease during the ignition stage but increase during the process of transition from a two-nozzle impinging to a four-nozzle one. With an increase in the operational load, the fractal dimension will also increase. However, the difference between the fractal dimension of a two-nozzle and four-nozzle impinging flames will gradually diminish. **Key words:** IGCC, impingement, gasification, flame, fractal characteristics

含盐有机废液焚烧煤灰熔融特性试验研究 = **Experimental Study of Coal-ash Fusion Characteristics Obtained from the Incineration of Salty Organic Waste Liquid** [刊, 汉] / CHEN Hui-chao, ZHAO Chang-sui, CHEN Xiaoping, et al (Education Ministry Key Laboratory on Clean Coal Power Generation and Combustion Technology under the Southeast University, Nanjing, China, Post Code: 210096) // Journal of Engineering for Thermal Energy & Power. — 2007, 22(1). — 61 ~ 64, 72

Studied are the ash fusion characteristics obtained from the mixed incineration of 1. three types of coal (Yuanbaoshan-origin lignite, Cuijiagou-origin bituminous coal and Xuzhou bituminous coal, hereinafter referred to as Coal Y, Coal C and Coal X for short respectively), which have different ash fusion characteristics, and 2. chemical waste-liquid red water with different salt contents (the content of alkali metal sodium salt Na_2SO_4 , NaNO_3 and Na_2CO_3 etc. in red water, hereinafter generally referred to as the salt content). The study results show that if no limestone is added, the ash fusion tem-